

DOI: <https://doi.org/10.24297/jap.v18i.8881>

## Synthesis on Heavy Higgs from the Standard Model to 2HDM and Beyond

A. Habjia<sup>a\*</sup><sup>a</sup>Physics department FST - Béni Mellal, Sultan Moulay Slimane University - Morocco.

habjia.a@ucd.ac.ma

### Abstract:

In the context of particle physics, within the ATLAS and CMS experiments at large hadron collider (LHC), this work presents the discussion of discovery a particle compatible with the Higgs boson by the combination of several decay channels, with a mass of the order of 125.5 GeV. With an increased statistics, that is the full set of data collected by the ATLAS and CMS experiments at LHC ( $\sqrt{s} = 7\text{GeV}$  and  $\sqrt{s} = 8\text{GeV}$ ), the particle is also discovered individually in the channel  $h \rightarrow \gamma\gamma$  with an observed significance of  $5.2\sigma$  and  $4.7\sigma$ , respectively. The analysis dedicated to the measurement of the mass  $m_h$  and signal strength  $\mu$  which is defined as the ratio of  $\sigma(pp \rightarrow h) \times Br(h \rightarrow X)$  normalized to its Standard Model where  $X = WW^*; ZZ^*; \gamma\gamma; gg; f\bar{f}$ . The combined results in  $h \rightarrow \gamma\gamma$  channel gave the measurements :  $m_h = 125.36 \pm 0.37\text{GeV}$ , ( $\mu = 1.17 \pm 0.3$ ) and the constraint on the width  $\Gamma(h)$  of the Higgs decay of 4.07 MeV at 95%CL. The spin study rejects the hypothesis of spin 2 at 99 %CL. The odd parity (spin parity  $0^-$  state) is excluded at more than 98 %CL. Within the theoretical and experimental uncertainties accessible at the time of the analysis, all results : channels showing the excess with respect to the background only hypothesis, measured mass and signal strength, couplings, quantum numbers ( $J^{PC}$ ), production modes, total and differential cross-sections, are compatible with the Standard Model Higgs boson at 95%CL. Although the Standard Model is one of the theories that have experienced the greatest number of successes to date, it is imperfect. The inability of this model to describe certain phenomena seems to suggest that it is only an approximation of a more general theory. Models beyond the Standard Model, such as 2HDM, MSSM or NMSSM, can compensate some of its limitations and postulate the existence of additional Higgs bosons.

**keywords:** Higgs Boson ; Standard Model ; LHC ; ATLAS ; CMS ; diphoton; 2HDM; MSSM; NMSSM.

### 1. Introduction

Particle physics is concerned with describing the structure of matter by studying its elementary components and their interactions. It is also known as high-energy physics because a large number of particles that existed in the first moments after the Big Bang can today only be created using high-energy particle collisions. The Standard Model of Particle Physics is the theoretical framework, set up in the second half of the 20th century, to classify particles and understand their interactions. Its parameters have been verified experimentally with great precision. Using the Higgs mechanism, predicted in 1964 by the physicists Brout, Englert [1] and Higgs [2], this model makes it possible to explain the origin of the mass of the bosons W and Z, while retaining a



mass zero at the photon; it thus breaks the gauge symmetry of the electroweak interaction. This mechanism is associated with a residual particle, the Higgs boson.

Despite the incredible success of this theory, the Standard Model fails to fully describe the fundamental interactions. In order to refine the precision of the parameters of this theory, to try to highlight the Higgs boson and to test models beyond the Standard Model, physicists built an accelerator of giant particles, 27 km in circumference, buried 100 m underground: the Large Hadron Collider (LHC) at CERN. The latter accelerates heavy ions but also and above all proton beams and makes them collide. Around these collision points, there are seven experiments including ATLAS (A Toroidal LHC ApparatuS) and CMS (Compact Muon Solenoid), two generalist detectors. These detectors have been specially designed to highlight the Higgs boson. The last experimental results highlight the existence of a scalar boson of zero spin having a mass of 125.5 GeV and compatible with the Higgs boson of the Standard Model. My work is a discussion of the discovery of the Higgs boson in the canal  $h \rightarrow \gamma\gamma$ . we propose a panorama of the Standard Model of particle physics and its theoretical construction based on gauge theories. The Brout-Englert-Higgs mechanism allowing spontaneous symmetry breaking is exposed, followed by the phenomenology of the Higgs boson. A non-exhaustive review of the success of the Standard Model is presented, as well as experimental observations suggesting the existence of physics beyond. Different results are presented, in particular the combination at different energies and luminosities, as well as the combined results of the measurement of the Higgs couplings with the other particles.

## 2. Overview of Standard Model and beyond

in this section, we will first present the theoretical framework of the Standard Model (MS). To do this, we will see what are the elementary particles and how they interact with each other and introduce mathematical formalism. We will then return in more detail to the Higgs mechanism allowing us to break the symmetry of the electroweak interaction, as well as to its scalar boson. In a third sub-section, we will describe the state of research on the Higgs boson after the discovery of a scalar Higgs boson. At the end, it will be devoted to the presentation of models beyond the MS, among which the 2HDM.

### 2.1. Elementary particles

By elementary constituents, we mean non-composite at the scale of the processes considered. Indeed, in the MS, the particles are considered to be punctual and without any underlying structure. Over the centuries, the number of these constituents has changed a lot. These changes are strongly correlated with technological progress allowing us to reach ever smaller distances (around  $10^{-18}$  m with the LHC). Each great revolution in physics is accompanied by a sharp reduction in the number of elementary particles. The MS, to which we refer today, has thirty-six. Its constituents can be separated into two main categories according to their intrinsic angular momentum (spin). On the one hand we have fermions, particles of matter, having a half integer spin. On the other, with their entire spin, we find the bosons whose mediators of fundamental interactions.

## 2.2. Fermions

The Standard Model includes twelve particles of the spin  $1/2$ . They obey Fermi's statistics where their name comes from and thus respect the Pauli exclusion principle. There are two types of fermions: leptons, insensitive to strong interaction and quarks, participating in all interactions. Each of these particles is associated with an antiparticle having an identical mass and spin but opposite internal quantum numbers (notably the electric charge).

## 2.3. Leptons

The most famous of the leptons is the electron. The latter is notably responsible for the chemical properties of atoms and is involved in most of the electromagnetic phenomena of our daily life. We can classify leptons into three families (or three lepton flavors), each with an electrically charged particle (the electron is one of them) and a neutral particle (neutrino). Their main characteristics are summarized in the Table 1. We thus find the electron ( $e^-$ ), the muon ( $\mu^-$ ) and tau ( $\tau^-$ ) with electrical charges of  $-1.6 \times 10^{-19}C$ , sensitive to electromagnetic interaction, and respectively their three associated neutrinos: the electronic neutrino ( $\nu_e$ ), the muonic neutrino ( $\nu_\mu$ ) and the tau neutrino ( $\nu_\tau$ ). They all have a leptonic number which has so far been kept in all interactions.

Table 1. Example of a table showing that its caption is as wide as the table itself and justified.

Names	Discovery	Mass (MeV)	Electrical charge	Spin	Antiparticle
$e$	1897(1932 $\bar{e}$ )	0.511	-1	1/2	$e^+$
$\nu_e$	1956	$\leq 10^{-6}$	0	1/2	$\bar{\nu}_e$
$\mu$	1937	105.66	-1	1/2	$\mu^+$
$\nu_\mu$	1962	$\leq 0.19$	0	1/2	$\bar{\nu}_\mu$
$\tau$	1975	1776.92	-1	1/2	$\tau^+$
$\nu_\tau$	2000	$\leq 18.2$	0	1/2	$\bar{\nu}_\tau$

Unlike the electron, the muon and tau are unstable and can decay into particles of other families via the weak interaction. Neutrinos do not interact by electromagnetic interaction but essentially by weak and gravitational interaction. As a result, reactions with the rest of the material are very rare. The precise measurement of the width of the  $Z$  boson at LEP made it possible to constrain the number of light neutrinos to three [9]. They have long been considered massless, but recent experiences (Super-Kamiokande [10], CHOOZ [11], Opera [12], T2K [13]) have shown that they can oscillate; that is, turning into neutrinos from other families. As a result, their mass cannot be zero and a lot of effort is made to constrain them. Another interesting feature of neutrinos is that they could be so-called "Majorana" particles, that is, be their own antiparticle (like the photon).

### 2.4. Quarks

The increased energy in  $e^+e^-$  collisions made it possible to highlight the different flavors of the quarks. The Standard Model now has six quarks. The last to be discovered is the top quark, in 1995 at the Tevatron [17,18]. The different levels in Figure 1, representing the ratio of the cross sections  $R = \sigma(e^+e^- \rightarrow \mu^+\mu^-)/\sigma(e^+e^- \rightarrow \text{hadrons})$  as a function of the energy in the center of mass, show that as the leptons, quarks are organized into three families. The masses of quarks as we can see in the Table 2 grow with the family and have very different orders of magnitude, the lightest quarks up, is about 75000 times lighter than the top quark. However, the mass of hadrons comes mainly from the strong interaction and not from that of the quarks.

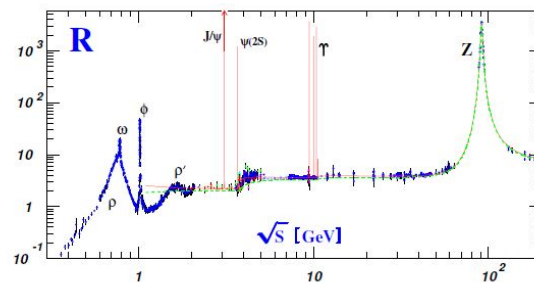


Figure 1.  $R = \sigma(e^+e^- \rightarrow \mu^+\mu^-)/\sigma(e^+e^- \rightarrow \text{hadrons})$  as a function of the energy in the center of mass  $\sqrt{s}$

Inside these composite particles, we find the so-called valence quarks which determine the quantum numbers of hadrons. In addition, each hadron can contain an indefinite number of virtual quarks (sea quarks), antiquarks and gluons (mediators of strong interaction) that have no influence on their quantum numbers. Finally, quarks are the only particles sensitive to the three fundamental interactions and have a quantum number called baryonic number conserved additively by all interactions.

Table 2. Characteristics of the three families of quarks of the Standard Model [14]

Names	Discovery	Mass (MeV)	Electrical charge	Spin	Antiparticle
$u$	1969	2.3	+2/3	1/2	$\bar{u}$
$d$	1969	4.8	-1/3	1/2	$\bar{d}$
$c$	1969	1275	+2/3	1/2	$\bar{c}$
$s$	1974	95	-1/3	1/2	$\bar{s}$
$t$	1995	173070	+2/3	1/2	$\bar{t}$
$b$	1977	4180	-1/3	1/2	$\bar{b}$

We have seen that when counting their antiparticles, fermions have 24 elements. However, all the objects of our daily life consist essentially of the particles of the first family, namely: the electron and the quarks up and down, composing the protons and neutrons. The other, more massive particles are created by accelerators as well as in collisions of highly energetic particles (from cosmic rays) in the Earth’s atmosphere. The particles thus produced then disintegrate into lighter particles, of the first family.

## 2.5. The gauge bosons

In the Standard Model, quantified fields are associated with particles to serve as a support for the description of the three fundamental interactions. These describe the way in which the particles influence each other. These forces are created by the exchange of gauge bosons, most commonly in the form of virtual particles (particles whose effects are not measurable but which exist for a limited time). As these mediators (propagators) are bosons (integer spin), they obey the Bose-Einstein statistics. The characteristics of its bosons are summarized in the Table. 3.3. Before going any further, let's briefly detail these three interactions.

Table 3. Characteristics of the bosons (vectors) in the Standard Model [14]

Names	Discovery	Mass (GeV)	Electrical charge	Life time (s)
$\gamma$	1923	0	0	stable
$W^{\pm}$	1983	80.389	$\pm 1$	$10^{-25}$
$Z$	1983	91.457	0	$10^{-25}$
$8g$	1979	0	0	stable

## 2.6. Electromagnetic interaction

It is described within the Standard Model by quantum electrodynamics (QED), is mediated by the photon. This massless boson has a spin 1 and only couples to electrically charged particles while retaining the hadronic flavors and the three lepton quantum numbers. It spreads in a vacuum at the speed  $c = 299792458m/s$ . Coulomb phenomena are the result of exchanges of virtual photons. The radiation meanwhile corresponds to the emission of real photons. The electromagnetic interaction is of infinite range and is associated with the fine structure constant  $\alpha = e^2/4\pi = 1/137$ , which allows you to express its intensity. In reality, this constant is not really constant since it varies with energy.

## 2.7. Weak interaction

It is responsible for radioactive decays. It acts in particular during decay  $\beta$ , by the exchange of bosons  $W^+$ ,  $W^-$  to which is added the boson  $Z$ . Even if they are not necessarily generated, neutrinos are the signatures of this interaction. All particles except the gluons are sensitive to this interaction. It is at the origin of the change in flavor of the particles by the exchange of the  $W^+$  or  $W^-$  bosons. Unlike photons, the weak interaction mediating bosons are very massive and therefore limit its range. These masses have been measured with great precision at LEP and Tevatron: 80.389 GeV for  $W$  [20] and 91.457 GeV for  $Z^0$  [21]. The weak interaction also has a coupling constant  $g^2/4\pi = \alpha/\sin^2\theta_W$  where  $\theta_W$  is the Weinberg angle and is  $\sin\theta_W = 0.231$ .

## 2.8. *Strong interaction*

It maintains the link between the quarks inside the hadrons. Its residual effect is also at the origin of the cohesion of the nuclei. The mediators of this interaction are the gluons, 8 in number, first brought to light in 1979 at DESY [22]. They are, like the photon, massless and spin 1. Like quarks, gluons are colored objects, playing a role analogous to the electric charge. This attraction of color increases with distance and forces the quarks to be confined inside the hadrons. The coupling constant of the strong interaction is noted  $\alpha_s$  and depends on the pulses set play in reactions.

## 2.9. *Higgs Boson*

The Higgs boson is the last piece of the Standard Model. This boson is associated with the Higgs field, responsible for the spontaneous symmetry breaking of the electroweak interaction which notably explains why the  $W^\pm$ ,  $Z$  bosons are massive and the photon is not. It is the only scalar particle (spin 0) of the Standard Model and is therefore part of the bosons. This boson is itself massive and can be paired with other Higgs bosons. As we will see below, a boson with characteristics very close to the latter was discovered by the ATLAS and CMS collaborations. If we consider that this particle is indeed the Higgs boson of the Standard Model, then its mass would be about 125.5 GeV [14].

## 2.10. *Mathematical formalism*

In the Standard Model, the particles are associated with  $\Phi(x)$  fields depending on the space-time coordinates. These fields contain all the information about the particles they represent and can be seen as probability waves. As we saw previously, we only consider fields with spins 0, 1/2 or 1 (no spin 2 for gravity), the only ones with which we are able to write a coherent quantum theory of fields. Their dynamics are determined by an action  $\mathcal{S}$  described from a Lagrangian with four dimensions:

$$\mathcal{S}(\Phi) = \int \mathcal{L}(\Phi, \partial_\mu \Phi) \quad (1)$$

## 2.11. *The Lagrangian of the Standard Model*

The Lagrangian describes the interacting particles. It can be written as a sum of monomials depending on the fields and their derivatives. It breaks down into two main terms:

- A free Lagrangian  $\mathcal{L}_{libre}$  containing linear and bilinear terms of the fields, which describes the free propagation of the fields and defines their dimension in energy.
- A interaction Lagrangian  $\mathcal{L}_{int}$  where we find terms with at least three fields, which takes into account

the interactions between the fields.

The strength of an interaction is characterized by its coupling constant  $\alpha$ . In a disturbing regime, the amplitude of physical processes can be expressed as an expansion of  $\mathcal{L}_{int}$  with increasing order terms in  $\alpha$  which are represented by a set of Feynman diagrams. If  $\alpha$  is small enough, we can keep only the diagrams in order zero (tree level). In order to increase the accuracy, it is necessary to add to the calculation diagrams in the order of a loop. Finally, the Lagrangian can be written as a sum of monomials depending on the fields and their derivatives at a particular point of space.

$$\mathcal{L} = \sum_k c_k \mathcal{O}_k(x) = \mathcal{L}_{libre} + \mathcal{L}_{int} \quad (2)$$

However, the higher order diagram calculation can generate divergences (Ultraviolet or infrared). To solve this problem, a set of techniques known as renormalization has been implemented by Hollik, Denner. Thus, for each divergence we add a counter term in the initial Lagrangian. The dimension of the coefficients  $c_k$  in equation 2 determines the properties of the corresponding interaction. If we ask  $c_k = 1/\Delta^D$  where  $\Delta$  is an energy scale, we notice that the terms of dimension negative (with  $D > 0$ ) are non-renormalizable. They are only low energy, where their role is removed by a factor  $(E/\Delta)^D$ , but become important at high energy and make the theory non-perturbative. It is therefore imperative to write the Lagrangian using renormalizable interactions.

To write the Lagrangian of a theory, we must also choose the symmetries that leave it invariant. Global symmetries, which do not depend on the space point, constrain possible interactions. As for local symmetries, they lead to new interactions with gauge fields. Experimental observations have made it possible to constrain the choice of the Standard Model symmetry group to the following group:

$$U(1)_Y \times SU(2)_L \times SU(3)_C \quad (3)$$

$U(1)_Y \times SU(2)_L$  describes the electroweak interaction. Linear combinations of its generators make it possible to create the photons as well as the  $W^\pm$  and  $Z$  bosons. The fields associated with particles can be written as a sum of right  $\Phi_R$  and left  $\Phi_L$  components. The electroweak interaction is known to violate the parity and acts only on the left fields, from where the presence of the index  $L$  in  $SU(2)_L$ , the  $Y$  corresponds to the weak hypercharge, a conserved quantum number, connecting the electric charge and the third component of the weak isospin. We will now make a more detailed description of the Lagrangian of the Standard Model, considering only one family in order to simplify the equations.

$$q_L = \begin{pmatrix} u_L \\ d_L \end{pmatrix}, u_R, d_R, \ell_L = \begin{pmatrix} \nu_L \\ e_L \end{pmatrix}, e_R, (\nu_R) \quad (4)$$

with

$$\Phi_{L(R)} = P_{L(R)}\Phi = \frac{1}{2}(1 - (+)\gamma_5)\Phi \tag{5}$$

We can decompose the Lagrangian into four parts:

$$\mathcal{L} = \mathcal{L}_{cin} + \mathcal{L}_{bos} + \mathcal{L}_{Yuk} + \mathcal{L}_{Higgs} \tag{6}$$

**2.12. Kinematics of fermions**

This sector is known as Lagrangien de Dirac. It reflects the free propagation of fermions, but also their interactions with gauge bosons. It is written as follows:

$$\begin{aligned} \mathcal{L}_{cin} = & i\bar{\ell}_L\gamma^\mu D_\mu\ell_L + i\bar{e}_R\gamma^\mu D'_\mu e_R + i\bar{\nu}_R\gamma^\mu\partial_\mu\nu_R \\ & + i\bar{q}_L\gamma^\mu D_\mu q_L + i\bar{d}_R\gamma^\mu D''_\mu d_R + i\bar{u}_R\gamma^\mu\partial_\mu u_R \end{aligned} \tag{7}$$

where the covariant derivatives are expressed in this way:

$$\begin{aligned} D_\mu = & \partial_\mu + ig_2 T^a W_\mu^a + ig_1 Y(\ell_L/q_L) B_\mu, \quad \text{for } q_L/\ell_L \\ D'_\mu = & \partial_\mu + ig_1 Y(e_R) B_\mu, \quad \text{for } e_R \\ D''_\mu = & \partial_\mu + ig_s T_s^a G_\mu^a + ig' Y(d_L) B_\mu, \quad \text{for } q_R \end{aligned} \tag{8}$$

where  $g_1$  corresponds to the coupling of  $U(1)$  and  $B_\mu$  to the associated gauge boson.  $T^a = \sigma^a/2$  with  $\sigma^a$  matrices of Pauli, and  $W_\mu^1, W_\mu^2, W_\mu^3$  are respectively the three generators and bosons of gauge of  $SU(2)$  with  $g$  its coupling;  $g_s$  is the strong coupling,  $T_s^a$  the generators of  $SU(3)$  and  $G_\mu^a$  the fields corresponding to the gluons.  $Y(f)$  is the hypercharge of the fermion  $f$ . The  $W_\mu^a$  and  $B_\mu$  fields are not physical, but their combinations make it possible to form the gauge bosons:

$$\begin{aligned} W^\pm = & \frac{1}{\sqrt{2}}(W_\mu^1 \pm iW_\mu^2) \\ Z_\mu = & \cos\theta_W W_\mu^3 - \sin\theta_W B_\mu \\ A_\mu = & \cos\theta_W B_\mu + \sin\theta_W W_\mu^3 \end{aligned} \tag{9}$$

The kinetic term for gauge bosons, or Yang Mills term, is expressed as follows:



$$\mathcal{L}_{bos} = -\frac{1}{4}B_{\mu\nu}B^{\mu\nu} - \frac{1}{4}F_{\mu\nu}^a F^{a\mu\nu} - \frac{1}{4}F_{\mu\nu}^A F^{A\mu\nu} + \mathcal{L}_{fix.jauge} + \mathcal{L}_{FPghosts} \quad (10)$$

with

$$B_{\mu\nu} = \partial_\mu B_\nu - \partial_\nu B_\mu, \quad \text{and} \quad F_{\mu\nu}^a = \partial_\mu A_\nu^a - \partial_\nu A_\mu^a - gf^{abc}A_\mu^b A_\nu^c \quad (11)$$

$B_{\mu\nu}$  is the Yang Mills tensor,  $F_{\mu\nu}^a$  ( $a=1,2,3$ ) the weak interaction tensor, associated with the gauge bosons of  $SU(2)$ , and  $F_{\mu\nu}^A$  ( $A=1,\dots,8$ ) the tensor of the strong interaction. In order to be able to make a perturbative calculation, additional terms of gauge fixation and Faddeev-Popov ghosts must be added.

### 2.13. Higgs term

The Higgs Lagrangian contains a potential which spontaneously breaks the symmetry of the electroweak interaction by generating masses for the bosons of gauge  $W^\pm$  and  $Z$

$$\mathcal{L}_{Higgs} = |D_\mu \Phi|^2 - \mu^2 (\Phi^\dagger \Phi) - \lambda (\Phi^\dagger \Phi)^2 \quad (12)$$

where  $\mu^2$  and  $\lambda$  are two free, real and constant parameters.

## 3. The Higgs boson of the Standard Model

### 3.1. Spontaneous breaking symmetry of the electroweak interaction

By choosing the parameters  $\mu^2 < 0$  and  $\lambda > 0$ , the Higgs potential has its minima on the surface.

$$|\Phi|_{\min}^2 = -\frac{\mu^2}{2\lambda} = \frac{v^2}{2} \quad (13)$$

with  $v^2 = -2\frac{\mu^2}{\lambda}$ . We will choose the vacuum

$$\langle 0|\Phi|0\rangle = \begin{pmatrix} 0 \\ \frac{v}{\sqrt{2}} \end{pmatrix} \quad (14)$$

and configure the fields around this vacuum with

$$\Phi = \exp\left(\frac{i}{v}\xi_i(x)\sigma_i\right) \begin{pmatrix} 0 \\ \frac{v+h(x)}{\sqrt{2}} \end{pmatrix} \quad (15)$$

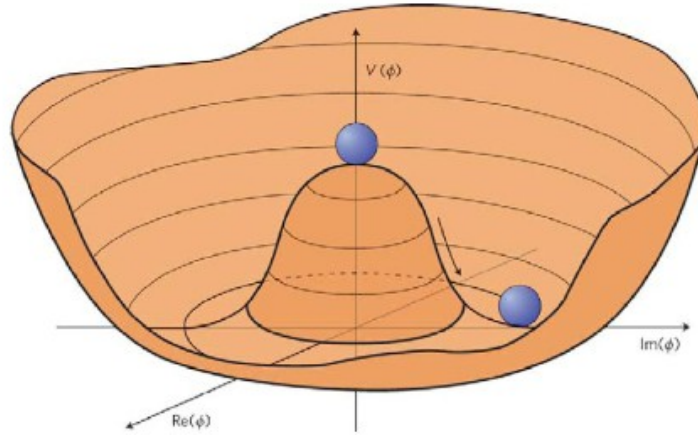


Figure 2. The scalar potential of the Standard Model

where we introduced the fields  $\xi_i(x)$  ( $i=1,2,3$ ) and  $h(x)$  which cancel out in a vacuum. The unitary phase matrix  $U(x)$  is a gauge transformation of  $SU(2)$  which gives us directly the results in the unitary gauge. The corresponding gauge transformation on the  $SU(2)_L$  gauge fields is found by looking at the covariant derivative:

$$\begin{aligned} D_\mu \Phi &= \left(\partial_\mu + i\frac{1}{2}W_\mu^a T_a + \frac{i}{2}B_\mu\right) U(x) \begin{pmatrix} 0 \\ \frac{v+h(x)}{\sqrt{2}} \end{pmatrix} \\ &= U(x)U^\dagger(x) \left(\partial_\mu + i\frac{1}{2}W_\mu^a \tau_a + \frac{i}{2}B_\mu\right) U(x) \begin{pmatrix} 0 \\ \frac{v+h(x)}{\sqrt{2}} \end{pmatrix} \\ &= U(x) \left(\partial_\mu + i\frac{1}{2}W_\mu^a \tau_a + \frac{i}{2}B_\mu\right) \begin{pmatrix} 0 \\ \frac{v+h(x)}{\sqrt{2}} \end{pmatrix} \end{aligned} \quad (16)$$

where the last equality is obtained by taking  $W'_\mu = -iU^\dagger(x)\partial_\mu U(x) + U^\dagger(x)W_\mu U(x)$ , so that the matrix  $U(x)$  disappears completely from the Lagrangian:

$$\begin{aligned} \mathcal{L}_{Higgs} &= \frac{1}{2}\partial_\mu h\partial^\mu h + \frac{1}{2}(B_\mu - W_{3\mu})(B^\mu - W_3^\mu)(v+h)^2 \\ &\quad + \frac{1}{8}(W_{1\mu} - iW_{2\mu})(W_1^\mu + iW_2^\mu)(v+h)^2 \\ &\quad + \lambda v^2 h^2 + \lambda v h^3 + \frac{\lambda}{4}h^4 - \frac{\lambda}{4}v^2 \end{aligned} \quad (17)$$

We can read the term mass for the Higgs boson

$$\lambda v^2 h^2 = \frac{1}{2} m_h^2 h^2, \quad \text{so we have} \quad m_h^2 = 2\lambda v^2 \quad (18)$$

but it is difficult to read the terms of mass for the bosons of gauge because of the terms mixing. Appropriate linear combinations of fields must be defined to eliminate mixing terms between gauge bosons. Before, we will reintroduce the coupling constants that were hidden in the fields.

$$B_\mu \rightarrow g_1 B_\mu, \quad W_\mu \rightarrow g_2 W_\mu, \quad A_\mu^A \rightarrow g_3 A_\mu^A \quad (19)$$

We can verify that with this definition, the kinetic terms of the gauge fields, take the usual form of the equation 10

$$\mathcal{L}_{YM} = -\frac{1}{4} B_{\mu\nu} B^{\mu\nu} - \frac{1}{4} W_{\mu\nu}^a W^{a\mu\nu} - \frac{1}{4} F_{\mu\nu}^A F^{A\mu\nu} \quad (20)$$

To find the diagonal shape of the masses, we impose in the loaded sector the relation:

$$m_W^2 W_\mu^+ W^{-\mu} \equiv \frac{g_2^2 v^2}{8} (W_{1\mu} - iW_{2\mu}) (W_1^\mu + iW_2^\mu) \quad (21)$$

and we have the mass of two loaded gauge bosons, which is:

$$m_W^2 = \frac{g_2^2 v^2}{4} \quad (22)$$

For gauge bosons neutral with respect to the electric charge, we must find a linear combination without mass which corresponds to the photon

$$\frac{1}{2} m_Z^2 Z_\mu Z^\mu + \frac{1}{2} 0 A_\mu A^\mu \equiv \frac{v^2}{8} (g_1 B_\mu - g_2 W_{3\mu}) (g_1 B^\mu - g_2 W_3^\mu) \quad (23)$$

this equation can be written according to a mass matrix

$$\frac{1}{2} (Z_\mu, A_\mu) \begin{pmatrix} m_Z^2 & 0 \\ 0 & 0 \end{pmatrix} \begin{pmatrix} Z^\mu \\ A^\mu \end{pmatrix} \equiv \frac{v^2}{8} (W_{3\mu}, B_\mu) \begin{pmatrix} g_2^2 & -g_1 g_2 \\ -g_1 g_2 & g_1^2 \end{pmatrix} \begin{pmatrix} W_3^\mu \\ B^\mu \end{pmatrix} \quad (24)$$

and the link between the two descriptions is made by an orthogonal transformation

$$\begin{pmatrix} Z^\mu \\ A^\mu \end{pmatrix} = \begin{pmatrix} \cos \theta_W & -\sin \theta_W \\ \sin \theta_W & \cos \theta_W \end{pmatrix} \begin{pmatrix} W_3^\mu \\ B^\mu \end{pmatrix} \quad (25)$$

with

$$\cos \theta_W = \frac{g_2}{\sqrt{g_1^2 + g_2^2}}, \quad \sin \theta_W = \frac{g_1}{\sqrt{g_1^2 + g_2^2}} \quad (26)$$

where  $\theta_W$  is the angle of Weinberg. The mass of the photon is zero and that of the boson  $Z$  is equal

$$m_Z^2 = \frac{v^2}{4} (g_1^2 + g_2^2) \quad (27)$$

The comparison between formulas 22 and 27 gives the relation, valid at the level of the tree

$$\frac{m_W^2}{m_Z^2} = \cos^2 \theta_W \quad (28)$$

#### 4. The decay channels of the Higgs boson

The coupling of the Higgs Standard boson with fermions is directly proportional to the fermionic masses and its coupling with the vector bosons goes like the square of the masses of the bosons. Since auto-coupling terms are present in the potential, interaction vertex with three or four Higgs bosons are possible. Equations 6, 12 and 18 give the coupling constants associated with these different processes:

$$\begin{aligned} g_{hf\bar{f}} &= \frac{m_f}{v}, & g_{hVV} &= \frac{2m_V^2}{v}, & g_{hhVV} &= \frac{2m_V^2}{v} \\ g_{hhh} &= \frac{3m_h^2}{v}, & g_{hhhh} &= \frac{3m_h^2}{v^2} \end{aligned} \quad (29)$$

where  $V = W^\pm, Z$ . grace to these couplings, the branching ratios (decay rate) of the different decay channels can be obtained as a function of the mass of the Higgs boson. This is what is shown in the Figure 3

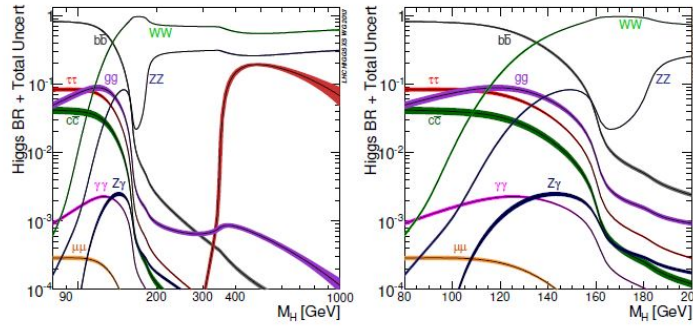


Figure 3. Branching ratios of the different decay channels of the Higgs Standard boson according to its mass

The dominant mechanisms involve the  $W^\pm, Z$  bosons as well as the third generation of quarks and leptons. For masses of the Higgs boson less than twice the mass of  $W$  or  $Z$ , the other lighter families have significant branching ratios. On the figure 3, we see that it is also possible to have two gluons or photons in the final state. Although massless, these bosons couple to the Higgs boson via  $t\bar{t}$  or  $W^+W^-$  loops. It is also possible for the Higgs boson to decay into a  $Z$  boson and a photon, again grace to massive particle loops like the  $W$  and the top quark. However, the existence of these loops means that the associated processes are strongly suppressed compared to the others. Thus, for a mass of the Higgs boson around 125.5 GeV, the branching ratio of  $h \rightarrow \gamma\gamma$  is in the range of  $2.1 \times 10^{-3}$ .

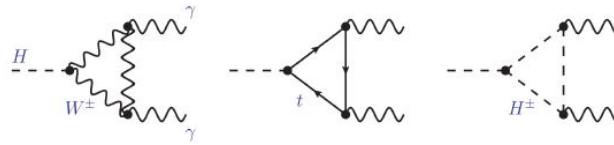


Figure 4. Example of a decay of  $h \rightarrow \gamma\gamma$  to the order of a one loop in the Standard Model as well as beyond (the third diagram).

### 4.1. Decay into two fermions

These processes give direct information on the coupling between the Higgs boson and the fermions. Indeed, the Higgs boson gives a fermion/antifermion pair without going through virtual particle loops, we say on the tree. In a hadronic collider, a very large number of jets (hadronic sprays) are created by QCD processes. It is therefore extremely difficult to study the decay of the Higgs boson into quarks, which is why experimenters most often favor lepton end states. However, several hadronic channels remain interesting due in particular to their high branching ratio. at low masses ( $<150$  GeV), this is the case of the events  $h \rightarrow b\bar{b}$  which represent 60% of the decays for a mass of 125.5 GeV. They can be identified grace to the relatively long life time of the quark  $b$ , thus producing displaced vertex, but also and above all using the additional leptons produced by the production mechanism  $VH$ . Also note the channel  $h \rightarrow \tau^+\tau^-$  which is good but very difficult to study because of the strong background noise (mainly  $Z\tau^+\tau^-$ ) makes it possible to probe the leptonic coupling. The other channels, due to their too low branching ratio, will only be really usable with a leptonic collider such as the International Leptonic Collider (ILC)  $e^+e^-$ .

#### 4.2. Decay into two massive bosons

Like fermions, these massive bosons couple directly to the Higgs boson. One of the major interests of these channels comes from their very large mass range. Above 150 GeV, these are the only channels usable at the LHC with the  $t\bar{t}$  channel, their branching ratios becoming ultra-majority. Even if its branching ratio is not the highest (30% after 200 GeV), the  $h \rightarrow ZZ$  is ideal for research at the LHC. Indeed, we can have four charged leptons in the final state (BR  $\sim 3\%$  at 125.5 GeV), which is a very clear signal in hadronic medium with little background noise ( $ZZ, Z\gamma$ ). It is then possible to reconstruct a narrow resonance in the invariant mass spectrum with four leptons. Other channels with two charged leptons and two quarks or missing transverse energy are also being studied, but have less sensitivity. The  $h \rightarrow W^+W^-$  channel has a very high branching ratio (70% after 200 GeV). The most interesting end state is obviously where we find two charged leptons. However, the missing transverse energy induced by the neutrinos prevents precise reconstruction of an invariant mass and therefore from seeing the appearance of a peak. In addition, this channel is accompanied by strong background noise, most of which comes from  $WW$  decays.

#### 4.3. $h \rightarrow \gamma\gamma$ decay

The Higgs boson can decay into two photons via one loop of vector bosons (see the first diagram in Figure 3) or top quarks (the second diagram in Figure 3). With the channel in four leptons,  $h \rightarrow \gamma\gamma$  is one of the most sensitive channels for low masses ( $m_h < 120$  GeV).

Although its branching ratio is very low, its interest comes from its very clear final state with two isolated high energy photons. This decay nevertheless has a relatively significant background noise:  $\gamma\gamma$  prompt QCD, misidentification of one or more neutral mesons and, as we will see below, poorly identified Drell Yan electrons around 90 GeV. In addition, as we see in Figure 5, the Higgs boson has a very small decay width for this mass range ( $\sim 5$  MeV at 125.5 GeV).

#### 4.4. $h \rightarrow Z\gamma$ decay

This process is very near to the decay  $h \rightarrow \gamma\gamma$ , since only one of the two photons of the final state is replaced by a  $Z$  boson. However, the probability for a loop of  $W$  or top quarks to emit a  $Z$  is lower. The branching ratio is thus very low ( $\sim 10^{-3}$  at 125.5 GeV) and becomes even more if we consider only the channel where the  $Z$  decays into two leptons. Even if studies on 13 TeV data are in progress course (with an integrated luminosity of  $20.5 fb^{-1}$ , significant sensitivity can only be obtained with high luminosity and higher energy in the center of mass.

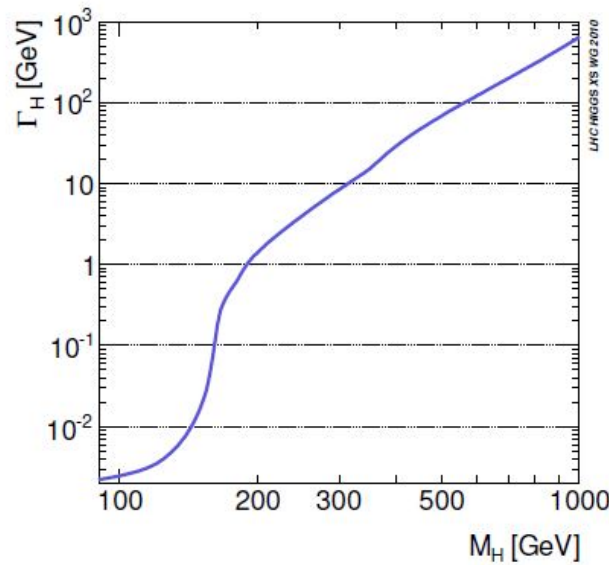


Figure 5. Total width of the Higgs boson in the Standard Model as a function of its mass  $m_h$ .

### 5. Higgs boson production at the LHC

Unlike the decaying processes of the Higgs boson, its modes of production depend both on the type of particles colliding and on their energy. At the LHC, there are four main channels: the fusion of gluons, the fusion of vector bosons, the Higgsstrahlung or associated production and the channel  $t\bar{t}h$ . Looking at the Figure 6 which represents the production cross sections of the Higgs boson as a function of its mass for an energy of 7 TeV in the center of mass, we can see that the dominant process is the fusion of gluons. At 125 GeV for example, the total production cross section is around 22 pb and is made up of more than 87% by gluon fusion. Analysis of the Figure 6 helps to understand where the predominance of this mechanism comes from at the LHC. In this figure is represented the ratio of partonic luminosity for different energies in the center of mass, as a function of the mass of the Higgs boson. What we immediately see is that the higher the energy, the greater the contribution of the gluons inside the protons compared to that of the quarks.

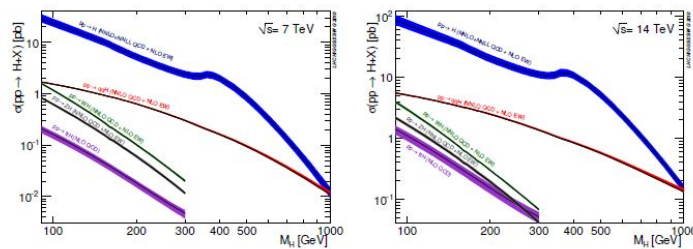


Figure 6. Cross section production of the Higgs boson at the LHC according to its mass  $m_h$ .

Another important point comes from the energy in the center of mass which greatly increases the production cross section of the Higgs boson. Thus, Figure 8. shows us that for a Higgs boson at 125 GeV, for an identical luminosity, having an energy in the center of mass of 14 TeV makes it possible to produce approximately

ten times more Higgs bosons than at an energy of 7 TeV. Although the modes of production can be studied separately, the extraction of the couplings of the Higgs boson with the different particles is particularly delicate (convolutions of several mechanisms). In some of these processes, particles are produced in association with the Higgs boson and make it easier to detect.

### 5.1. Gluon fusion

Produces a Higgs boson through a top quark loop (Figure 7). We thus obtain information on the coupling with the top, whose mass very high compared to that of the other quarks is an enigma. In addition, other massive particles, not yet discovered, may be involved in these loops. A fine measurement of the cross section of this process thus gives indications on the possibility of a new physics.

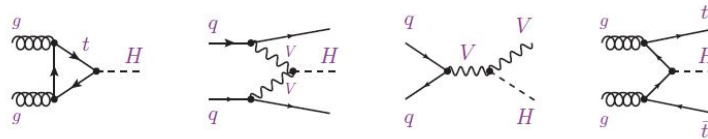


Figure 7. Cross section production of the Higgs boson at the LHC according to its mass  $m_h$ .

### 5.2. The fusion of vector bosons (VBF)

it is a particularly interesting mode of production since as we see using the 2nd diagram on the left of figure 7, the Higgs boson is produced jointly with two quarks. In the final state, we will therefore have, in addition to the decay products of the Higgs boson, two jets produced towards the front (with a small angle relative to the axis of the beams). Thus, although its cross section is ten times lower than the gluon fusion, events with this production mode have very little background noise.

### 5.3. The Higgsstrahlung

It has a cross section of the same order as the VBF channel, but this time the Higgs boson is emitted by a  $W$  or  $Z$  boson, like a bremsstrahlung photon the 3rd diagram in Figure 7. Besides the direct measurement of the coupling with the weak interaction bosons, the decay of  $W$  and  $Z$  into leptons gives a final state which is easy to identify. However, this leptonic channel has a cross section too small to hope alone to highlight a Higgs boson with current data.

### 5.4. $t\bar{t} \rightarrow h$ channel

shown in the diagram on the right in Figure 7, is similar to the VBF channel. A top couple antitop annihilates to give a Higgs boson while two other top quarks are produced forward. Consequently, a search for a Higgs



boson produced in association with six jets (or four jets +  $\ell\nu$ ) is possible, but its sensitivity is too reduced (with current statistics) given its very small cross section at 8 TeV ( $\sigma_{tth} \sim 0.1$  pb for  $m_h = 125$  GeV).

## 6. Discovery of a Higgs boson compatible with $h_{MS}$

On July 4, 2012 the ATLAS and CMS collaborations jointly announced the discovery of a boson decaying into two photons as well as two  $Z$  bosons and having a mass close to 126 GeV. As we will see, since that date, the increase in the usable integrated luminosity and the improvement of the various analyzes have made it possible to constrain the mass, the spin and the decay channels of this new particle.

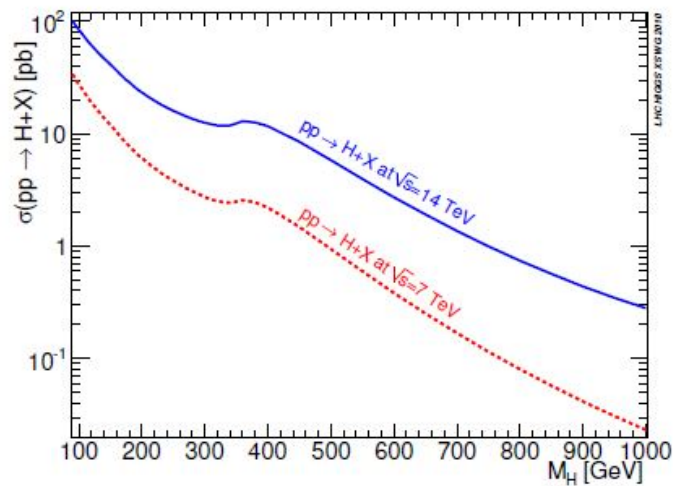


Figure 8. Cross section production of the Higgs boson at the LHC according to its mass for energies of 7, 8 and 14 TeV in the center of mass.

This discovery is not the only fruit of perfected analyzes but also of several theoretical constraints which made it possible to restrict the field of parameters.

### 6.1. Summary of constraints and compatibility with observation

Although the mass of the Higgs boson is not predicted by the Standard Model, there are upper and lower limits on its mass if we assume that there is no new physics between the electroweak scale and a higher energy scale called  $\Lambda$ .

### 6.2. Unitarity

As we mentioned before, without scalar field the amplitude of the elastic diffusions of the bosons  $W$ , polarized longitudinally, diverge like the square of energy in the center of mass. Calculated with our perturbative model for an energy of 1.2 TeV, these processes violate unitarity. When diagrams involving a scalar particle are

introduced into these diffusion processes, the divergences are no longer present and the theory remains unitary and renormalizable. Resolving these discrepancies constrains most of the properties of the Higgs boson. Thus, this divergence suppression mechanism only works if the Higgs boson is not too heavy. By requiring that our perturbative theory remain valid until  $\Lambda$ , an upper limit on the mass of the Higgs boson can be extracted. The non-violation of unitarity and the use of all the processes of diffusion of vector bosons gives

$$m_h \leq \sqrt{\frac{4\pi\sqrt{2}}{3G_F}} \sim 700\text{GeV} \quad (30)$$

where  $G_F$  is the Fermi constant, with  $G_F = 1.16637 \times 10^{-5}$ .

### 6.3. Triviality and stability of the vacuum

The auto interaction constant  $\lambda$  is used to predict high and low limits for the mass of the Higgs boson as a function of an energy scale  $\Lambda$ . The evolution of this constant with energy, considering only the couplings to a loop, is given by the following equation [27]:

$$\frac{d\lambda}{dt} = \frac{3}{4\pi^2} \left[ \lambda^2 + \frac{1}{2}\lambda y_t^2 - \frac{1}{4}\lambda y_t^4 + R(g_1, g_2) \right] \quad (31)$$

where  $t = \ln(Q^2)$  the impulse transfer,  $y_t$  the coupling of Yukawa Higgs-top and  $R_{(g_1, g_2)}$  a less important term including the contributions of the gauge bosons. With this expression, we can evaluate the value of  $\lambda(\Lambda)$  against a reference scale  $\lambda$ . To obtain limits on the mass of the Higgs boson, it is possible to study this function in two special regimes:  $\lambda \gg g_{1,2}$  or  $\lambda \ll g_{1,2}, y_t$ .

### 6.4. Indirect measures

It is possible to carry out a global adjustment of the electroweak parameters, where only the mass of the Higgs boson is a free parameter. Figure 10 representing  $\Delta_{\chi^2}$  of this global adjustment as a function of the mass of the Higgs boson, indicates that the Higgs boson must be light. Indeed, for two different values of the mass of  $W$ , the minimum value of  $\Delta_{\chi^2}$  is obtained for a mass of the Higgs boson near to 95 GeV. The uncertainty on the mass of  $W$  is the predominant contribution in this adjustment. Thus, it is possible to estimate the mass of the Higgs boson by calculating the radiative corrections of orders greater than the mass of  $W$ . These corrections involve loop diagrams containing in particular the Higgs boson. By experimentally measuring the mass of  $W$ , we can thus obtain a prediction on the mass of the Higgs boson.

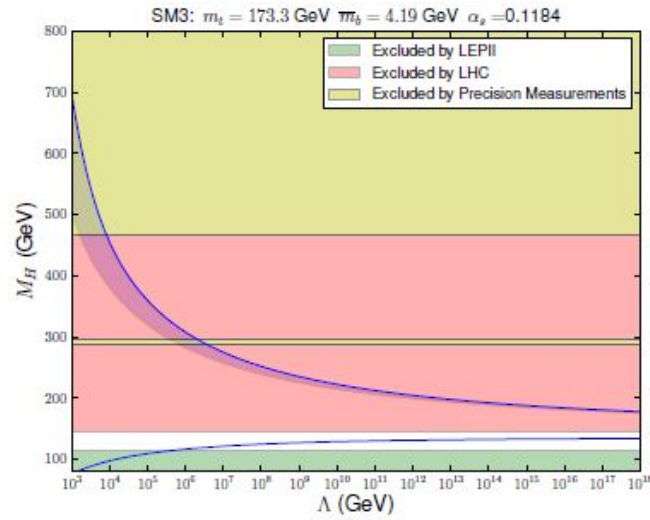


Figure 9. Stability and triviality of the potential of the Higgs boson in the Standard Model. The colors indicate the exclusion zones of LEP, LHC and the electroweak measurements.

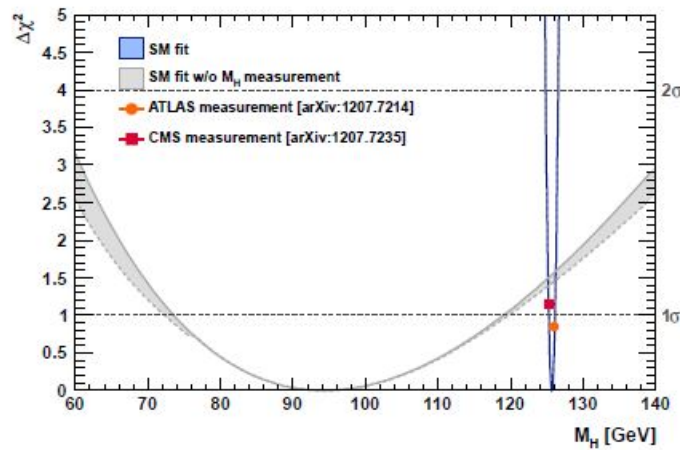


Figure 10. Distribution of  $\chi^2$  as a function of the mass of the Higgs boson, resulting from an overall adjustment of the parameters of the Standard Model, where only the mass of the Higgs boson is a free parameter.

### 6.5. Experimental results

The theoretical constraints and the electroweak precision measurements that we have just described made it possible to guide experiments in their search for the Higgs boson. In this section, we will describe their results and what they imply for this new particle. We will make a non-exhaustive list, presenting the main characteristics of this new boson and prioritizing the results of the ATLAS and CMS collaboration. The graphs which follow correspond to the combined results of the taps given at 7 TeV and 8 TeV, i.e. an integrated luminosity of  $5.1 + 19.1 \text{ fb}^{-1}$  for CMS and  $6 + 21 \text{ fb}^{-1}$  for ATLAS.

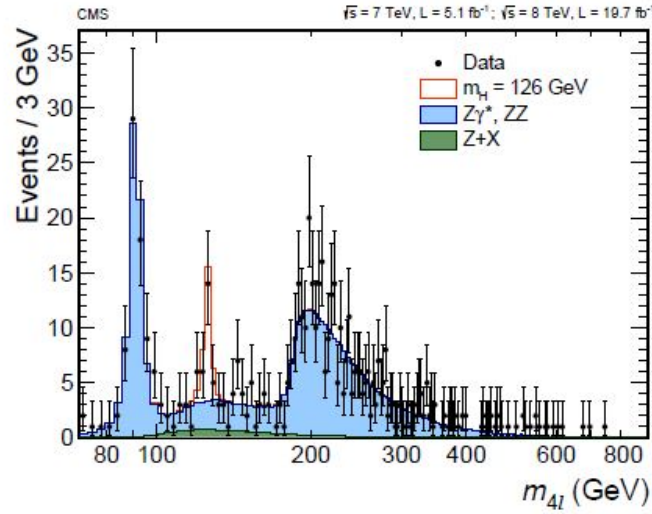


Figure 11. Distribution of the reconstructed invariant mass  $4\ell$ , combination of the 4 channels  $4\mu$ ,  $2e2\mu$  and  $4e$ .

### 6.6. Observation of excess in multiple channels

Due to their high branching ratio and / or their clear final state, the first physics analyzes focused on five modes of decay of the Higgs boson:  $h \rightarrow WW$ ,  $h \rightarrow ZZ$ ,  $h \rightarrow b\bar{b}$ ,  $h \rightarrow \tau^+\tau^-$  and  $h \rightarrow \gamma\gamma$ .

The most sensitive channel to 125 GeV is  $h \rightarrow ZZ \rightarrow 4\ell$ . Its final state comprising four charged leptons ( $4\mu$ ,  $2e2\mu$  or  $4e$ ), limpid in hadronic collider, makes it possible to reconstruct the invariant mass  $m_{4\ell}$  and to release the peak of the Higgs boson. This can be seen on the Fig. 11 where we can clearly see an excess compared to the background noise around 126 GeV. By placing itself in a low noise and signal regime, this study obtains an excellent signal to noise ratio. In order to increase the sensitivity of the analysis, a multivariate selection technique taking the kinematics of the input Higgs boson was used. If we calculate the ratio of the cross sections observed and predicted by the Standard Model ( $\mu$ ), we find for 125.6 GeV

$$\mu = 0.93_{-0.23}^{+0.26}(\text{stat})_{-0.09}^{+0.13}(\text{syst}) \quad (32)$$

the value compatible with a Higgs Standard boson. The other preferred disintegration channel is  $h \rightarrow \gamma\gamma$ . Here too, the diphoton invariant mass  $m_{\gamma\gamma}$  can be obtained, but the background noise being very high, a peak is more difficult to demonstrate. In fact, unlike channel  $h \rightarrow 4\ell$ , we place ourselves here in a regime with strong signal and background noise. It was therefore necessary to set up several boosted decision trees, in particular to select the correct vertices, photons and pairs of diphotons. To obtain better sensitivity, the events have been separated into nine subcategories. By assigning a weight to each event according to its category, it is possible to obtain a distribution  $m_{\gamma\gamma}$  with here again an excess with respect to the background noise around 126 GeV. The signal strength extracted by this analysis gives a result compatible with a Higgs Standard boson since

$$\begin{aligned} \mu &= 0.78 \pm 0.27 & \text{for } & CMS \\ \mu &= 1.13 \pm 0.17 & \text{for } & ATLAS \end{aligned} \tag{33}$$

Due to the missing transverse energy due to the neutrino, the reconstruction of an invariant mass in the three other analyzes provides little information. However, although we cannot see a clear peak, the distributions of the dilepton masses or of certain angular variables allow us to visualize an excess. In these three channels, the observed excesses are again compatible with a Higgs boson described by the Standard Model. For these five decay modes, the values of  $\mu$ , as well as the significance (probability that an excess is due to a fluctuation in the background noise), are summarized in the Table. 4.

Table 4. Significance and ratio of the observed cross sections divided by those of the Standard Model for the different decay channels of the Higgs boson.  $\rho$  is the correlation for each production mode.

$f$	$\hat{\mu}_{ggF+tth}^f$	$\hat{\mu}_{VBF+Vh}^f$	$\pm 1\hat{\sigma}_{ggF+tth}$	$\pm 1\hat{\sigma}_{VBF+Vh}$	$\rho$
$\gamma\gamma$	1.32	0.8	0.38	0.7	-0.30
$ZZ^*$	1.70	0.3	0.4	1.20	-0.59
$WW^*$	0.98	1.28	0.28	0.55	-0.20
$\tau\tau$	2	1.24	1.50	0.59	-0.42
$b\bar{b}$	1.11	0.92	0.65	0.38	0

The values of  $\mu$  obtained in the different decay channels can be combined in order to achieve an overall adjustment, that is to say, it is possible to extract and combine different  $\hat{\mu}^f$  ( $f = \gamma\gamma, ZZ^*, WW^*, \tau^+\tau^-$  and  $b\bar{b}$ ) corresponding to the main production channels of the Higgs boson  $ggF + tth$  and  $VBF + Vh$ . These adjustments give a value  $\hat{\mu}^{com} = 0.8 \pm 0.14$  for CMS, (compatible with less than  $2\sigma$  with the prediction of the Standard Model) and  $\hat{\mu}^{com} = 1.13 \pm 0.17$  for ATLAS (compatible with a  $1\sigma$  with the prediction of the Standard Model).

### 6.7. Higgs boson mass

The mass of this new state can be measured using the channels  $h \rightarrow ZZ \rightarrow 4\ell$  and  $h \rightarrow \gamma\gamma$  because they have a very good resolution (between 1 and 2%). Figure 12 shows the 68% confidence intervals at ATLAS and CMS for the two parameters that interest us, at know the signal strength  $\mu$  and mass of the new boson  $m_X$ . The black outline, symbolizing the 68% confidence interval for the combination of channels  $\gamma\gamma$  and  $4\ell$ , is obtained by supposing that the new particle corresponds to the Higgs boson of the Standard Model and by allowing the signal strength to fluctuate. Other methods, less related to the different models, have been carried out to extract the mass of this new state, assuming the independence of the signal strengths in the different channels. The result of these analyzes gives a mass

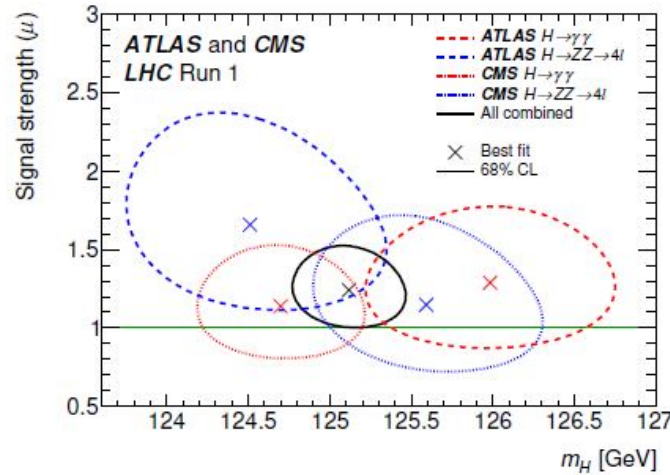


Figure 12. Contours representing the confidence interval of 68% CL for the signal strength as a function of the mass of the Higgs boson for the states  $\gamma\gamma$  and  $4\ell$  and for their combination.[31]

$$\begin{aligned}
 m_X &= 125.7 \pm 0.3(\text{stat}) \pm 0.3(\text{syst})\text{GeV} \quad (\text{CMS}) \\
 m_X &= 125.5 \pm 0.3(\text{stat})^{+0.5}_{-0.6}(\text{syst})\text{GeV} \quad (\text{ATLAS})
 \end{aligned}
 \tag{34}$$

### 6.8. Couplings with fermions and bosons

In order to test possible deviations between the data and the predictions of the Standard Model, for the different production and decay channels of the Higgs boson, it is possible to look at the couplings  $\kappa_i$  (normalized to the coupling of the Standard Model) (where  $i$  represents a fermion  $f$  or a vector boson  $V$ ) with the new particle and to carry out an adjustment on the data with these parameters (the couplings  $\kappa_i$  are the result of a particular parameterization [33]). Considering that there are no other modes of decay of the Higgs boson than those described by the Standard Model, then it is possible to explore the phase space  $\kappa_f, \kappa_V$ . Figure 13 shows the results of these adjustments for different Higgs boson decay channels and their combination. The data are compatible with a Higgs Standard boson since the point  $(\kappa_f, \kappa_V) = (1,1)$  is inside the 68% confidence interval defined by the data

## 7. The success of the Standard Model

As we have just stated, the Standard Model is an incomplete theory. Several of its characteristics are thus dictated by experience:

- Twenty-two non-predicted parameters: the masses of the six quarks and three charged leptons, three coupling constants, four mixture parameters for quarks and four for neutrinos, the mass of a vector boson and the mass of the boson of Higgs.

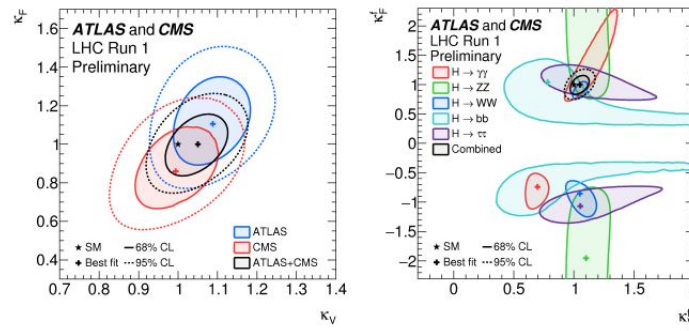


Figure 13. Confidence intervals at 68% for the different decay channels of the Higgs boson (colored areas) and their combination (black line), for the parameters  $\kappa_f$  and  $\kappa_V$ . [32]

- Although observations (notably the measurement of the width of the  $Z$  boson) have shown that it is very unlikely to have more than three families of particles on the electroweak scale, the Standard Model makes no prediction on this subject.

In addition to these gray areas, we know that the Standard Model does not explain all of the phenomena we know:

- It does not have a description of gravity although we know that quantum gravity effects must play a role on the Planck scale ( $10^{19}$  GeV). By simply adding a new particle, the graviton (without mass and spin 2), to the Standard Model to take into account gravitation, we realize that theory cannot describe gravity without deconstructing its other predictions. To date, there is no quantum field theory capable of integrating general relativity in a consistent manner (models integrating gravitation give no testable prediction).
- In the Standard Model, the mass of neutrinos is not naturally generated. However, neutrino oscillation experiments have shown that they must be massive. It is possible to add masses to neutrinos in the same way as for other fermions. Nevertheless, these new terms in the Lagrangian should be particularly weak; So much so that one wonders if the generation of the mass of neutrinos is not described by another process (Seesaw for example). The combined observations of the light emitted by spiral galaxies, clusters of galaxies and cosmological background noise, tell us that the universe must be composed at about 24% by dark matter, at 70% by energy black and only 4% by ordinary baryonic matter. The Standard Model only describes this 4%, but has no candidate particles for dark matter. Likewise, attempts to describe dark energy in terms of vacuum energy within this model have all failed.
- In the Standard Model, matter and antimatter are produced in equal quantities. So, shortly after the Big Bang, when the universe cooled down, particles and antiparticles should all have been annihilated in photons. However, today we live in a world of matter. There is therefore a material asymmetry (around  $10^9$ ) that no mechanism within the Standard Model can explain.

Finally, it is important to cite the problems more specifically linked to the Higgs boson. Indeed, despite the fact that the Higgs Mechanism makes it possible to resolve many tensions within the Standard Model, others

are associated with it:

- Since the Higgs field is present in all space, its non-zero value in vacuum must contribute to the energy of vacuum. For a Higgs boson with a mass of 126 GeV, the contribution of the Higgs field to the energy density of the vacuum should therefore be greater than  $10^8$  GeV [27]. However, cosmological measurements show that the energy density of the vacuum is about  $10^{46}$  GeV, a difference of fifty-four orders of magnitude.
- In the Standard Model, the mass of the Higgs boson must receive radiative corrections. However, the corrections from fermions (mainly from the top quark) are so important ( $\sim \Delta$ , the energy scale at which the theory ceases to be valid) that they far exceed the current mass of the Higgs boson. It therefore does not seem natural that the mass of the Higgs boson should be of the order of  $M_W$  rather than of  $\Delta$ . This is called the hierarchy problem which leads in the Standard Model to a fine adjustment of the parameters in order to cancel the contributions of the quark loops.

## 8. Two Higgs doublet models (2HDM)

In many aspect, the two Higgs doublet models (2HDM) can be seen as the simplest extension of the Standard Model with respect to the Higgs sector. Despite their simplicity, 2HDM are interesting because they can predict new phenomena such as spontaneous CP violation or even violation of the leptonic number. In these models, the Higgs sector is made up of two  $SU(2)_L$  doublets, instead of just one. These doublets interact through a potential that spontaneously breaks the symmetry of the electroweak interaction and generate three Goldstone bosons as well as five physical bosons (two charged and three neutral).

### 8.1. Higgs potential in 2HDM

In its most general form, the 2HDM contains two doublets of  $SU(2)_L$ :

$$\Phi_1 = \begin{pmatrix} \phi_1^+ \\ \phi_1^0 \end{pmatrix} (Y = +1/2), \quad \Phi_2 = \begin{pmatrix} \phi_2^0 \\ \phi_2^+ \end{pmatrix} (Y = -1/2) \tag{35}$$

Using these two fields, the invariant gauge and renormalizable potential can be written as follows [36]:

$$\begin{aligned} V_{2HDM} = & m_{11}^2 \Phi_1^\dagger \Phi_1 + m_{22}^2 \Phi_2^\dagger \Phi_2 - \left( m_{12}^2 \Phi_1^\dagger \Phi_2 + h.c \right) \\ & + \frac{\lambda_1}{2} \left( \Phi_1^\dagger \Phi_1 \right)^2 + \frac{\lambda_2}{2} \left( \Phi_2^\dagger \Phi_2 \right)^2 + \lambda_3 \left( \Phi_1^\dagger \Phi_1 \right) \left( \Phi_2^\dagger \Phi_2 \right) + \lambda_4 \left( \Phi_1^\dagger \Phi_2 \right) \left( \Phi_2^\dagger \Phi_1 \right) \\ & + \left\{ \frac{1}{2} \lambda_5 \left( \Phi_1^\dagger \Phi_2 \right)^2 + \left[ \lambda_6 \left( \Phi_1^\dagger \Phi_1 \right) + \lambda_7 \left( \Phi_2^\dagger \Phi_2 \right) \right] \left( \Phi_1^\dagger \Phi_2 \right) + h.c \right\} \end{aligned} \tag{36}$$



where  $m_{11}$ ,  $m_{22}$  and  $\lambda_i$  with  $i=1,2,3,4$  are real parameters due to the hermicity of the potential, while  $m_{12}^2$  and  $\lambda_{5,6,7}$  can be complex.

Unlike the case of the Standard Model, the gauge symmetry of the model is no longer sufficient to allow all the phases of the mean values to be eliminated simultaneously in the vacuum of the scalar fields. If the minimization conditions allow it, and as we will see in the next section, a spontaneous break of the CP symmetry cannot therefore be excluded, even in the context of an invariant potential such as 36. If one wishes to avoid this spontaneous break, it is therefore naturally necessary to require an additional symmetry. The first possibility is to impose a global symmetry  $U(1)$  additionally on one of the two doublets, i.e.  $\Phi_2 \rightarrow e^{i\Phi} \Phi_2$  makes it possible to "turn" the undesirable phase, it turns out however that this symmetry is wider than necessary. A simple  $\mathbb{Z}_2$  symmetry with  $\Phi_1 \rightarrow \Phi_1$  and  $\Phi_2 \rightarrow -\Phi_2$  is enough to prevent spontaneous breaking of the CP symmetry. The potential 36 then becomes:

$$\begin{aligned}
 V_{2HDM}(\Phi_1, \Phi_2) = & m_{11}^2 (\Phi_1^+ \Phi_1) + m_{22}^2 (\Phi_2^+ \Phi_2) - \{m_{12}^2 (\Phi_1^+ \Phi_2) + h.c\} + \frac{1}{2} \lambda_1 (\Phi_1^+ \Phi_1)^2 \\
 & + \frac{1}{2} \lambda_1 (\Phi_2^+ \Phi_2) + \lambda_3 (\Phi_1^+ \Phi_1) (\Phi_2^+ \Phi_2) + \lambda_4 (\Phi_1^+ \Phi_2) (\Phi_2^+ \Phi_1) \\
 & + \lambda_5 (\Phi_1^+ \Phi_2)^2 + \lambda_5^* (\Phi_2^+ \Phi_1)^2
 \end{aligned} \tag{37}$$

Such symmetry also ensures the absence of flavor-changing neutral currents (FCNC) by allowing each doublet to only couple to one type of fermion. Note that in the potential 37 we have tolerated the existence of the term  $m_{12}^2(\Phi_1^+ \Phi_2)$ , of dimension two, which sweet violates symmetry  $\Phi_1 \rightarrow \Phi_1$ ,  $\Phi_2 \rightarrow -\Phi_2$ . To best paste to the experimental results, we can impose constraints on the Lagrangian which make these effects impossible. There are several manners to do this, but we will describe here only one of them suggested by Weinberg and Glashow. The idea is to impose the following symmetry:

$$\mathbb{Z}_2 : \quad \Phi_1 \rightarrow \Phi_1, \quad \Phi_2 \rightarrow -\Phi_2 \tag{38}$$

## 9. Masses and couplings in 2HDM

### 9.1. The Higgs sector

In this paragraph, we are interested in the mass spectrum of 2HDM. Before tackling this, we give another parameterization of the potential of 2HDM which is equivalent to that of equation 37. We consider that the structure of doublets is written as follows:

$$\Phi_i = \begin{pmatrix} \phi_i^+ \\ \text{Re } \phi_i^0 + i \text{Im } \phi_i^0 \end{pmatrix} \quad i = 1, 2 \tag{39}$$

These fields are not physical fields, they do not have a well-defined mass. The next step is to diagonalize the mass matrix. We can see that the mass matrix is a diagonal matrix per block for the following components:  $\phi_1^+$ ,  $\phi_2^+$ ,  $\text{Re } \phi_1^0$ ,  $\text{Re } \phi_2^0$  and  $\text{Im } \phi_1^0$ ,  $\text{Im } \phi_2^0$ . Due to the conservation of CP, the real and imaginary parts can be treated separately. If we define the angle of rotation by:

$$R(\theta) = \begin{pmatrix} \cos \theta & \sin \theta \\ -\sin \theta & \cos \theta \end{pmatrix} \tag{40}$$

The fields are rotated to:

$$\begin{aligned} \begin{pmatrix} G^\pm \\ H^\pm \end{pmatrix} &= R(\beta) \begin{pmatrix} \phi_1^\pm \\ \phi_2^\pm \end{pmatrix} \\ \begin{pmatrix} H^0 \\ h^0 \end{pmatrix} &= \sqrt{2}R(\alpha) \begin{pmatrix} \text{Re } \phi_1^0 - v_1 \\ \text{Re } \phi_2^0 - v_2 \end{pmatrix} \\ \begin{pmatrix} G^0 \\ A^0 \end{pmatrix} &= \sqrt{2}R(\beta) \begin{pmatrix} \text{Im } \phi_1^0 \\ \text{Im } \phi_2^0 \end{pmatrix} \end{aligned} \tag{41}$$

with their masses:

$$\begin{aligned} m_{H^\pm}^2 &= \lambda_4 (v_1^2 + v_2^2) \\ m_{A^0}^2 &= \lambda_6 (v_1^2 + v_2^2) \\ m_{H^0, h^0}^2 &= \frac{1}{2} \left[ \mathcal{M}_{11} + \mathcal{M}_{22} \pm \sqrt{(\mathcal{M}_{11} - \mathcal{M}_{22})^2 + 4\mathcal{M}_{12}^2} \right] \end{aligned} \tag{42}$$

where  $\mathcal{M}_{ij}$  are the CP-even Higgs mass matrices

$$\mathcal{M} = \begin{pmatrix} 4v_1^2 (\lambda_1 + \lambda_3) + v_2^2 \lambda_5 & (4\lambda_3 + \lambda_5) v_1 v_2 \\ (4\lambda_3 + \lambda_5) v_1 v_2 & 4v_2^2 (\lambda_2 + \lambda_3) + v_1^2 \lambda_5 \end{pmatrix} \tag{43}$$

The  $\alpha$  and  $\beta$  mixing angles are:

$$\begin{aligned} \tan \beta &= \frac{v_2}{v_1} \\ \sin 2\alpha &= \frac{2\mathcal{M}_{12}}{\sqrt{(\mathcal{M}_{11} - \mathcal{M}_{22})^2 + 4\mathcal{M}_{12}^2}} \\ \cos 2\alpha &= \frac{\mathcal{M}_{11} - \mathcal{M}_{22}}{\sqrt{(\mathcal{M}_{11} - \mathcal{M}_{22})^2 + 4\mathcal{M}_{12}^2}} \end{aligned} \tag{44}$$

on the tree we get:

$$\frac{G_F}{\sqrt{2}} = \frac{g^2}{8M_W^2} \tag{45}$$

the value of v in the Standard Model

$$v = \sqrt{v_1^2 + v_2^2} = 246\text{GeV} \tag{46}$$

It is more practical to work with physical masses and mixing angles rather than with  $\lambda_i$ . We therefore choose as independent parameters:

$$4 \text{ masses} : m_{h^0}, m_{H^0}, m_{A^0}, m_{H^\pm}$$

2 mixing angles :  $\alpha, \beta$

$$\text{and : } \lambda_5 \quad \text{ou} \quad m_{12}^2 \tag{47}$$

### 9.2. The different types of 2HDM

Different 2HDM models exist in Table 5. For type-I, a doublet couplings with vector bosons, another with fermions. For type-II, a Higgs doublet couplings to high quarks, another to low quarks and leptons. Types X and Y differ in parameters specific to leptons. For Type-X, the Higgs bosons have the same quark couplings as type-I and the same lepton couplings as type-II. The Y model is an inverted model of X: the Higgs bosons have the same quark couplings as type-II and the same lepton couplings as type-I.

Thus, the observation of a resonance  $\phi$  in the  $\phi VV$  channel favors the hypothesis of an CP-even state since the coupling  $\phi VV$  by an CP-odd scalar state  $\phi$  can only exist in the state correction to the order of the loops.

$$\begin{aligned}
 -\mathcal{L}_Y = & \bar{U}_L \Phi_a^{0*} h_a^U U_R - \bar{D}_L K^\dagger \Phi_a^- h_a^U U_R + \bar{U}_L K \Phi_a^+ h_a^{D\dagger} D_R + \bar{D}_L \Phi_a^0 h_a^{D\dagger} D_R \\
 & + \bar{N}_L \Phi_a^+ h_a^{L\dagger} E_R + \bar{E}_L \Phi_a^0 h_a^{L\dagger} E_R + \text{h.c.}
 \end{aligned}
 \tag{48}$$

Supersymmetry requires being able to give masses for fermions in the up and down sector, which requires type-II, an example of which is the minimal supersymmetric model (MSSM). there are 3 gauge fields without mass  $W_{1,2,3}^\mu$  of  $SU(2)_L$  with two degrees of freedom each, a massless field  $B^\mu$  of  $U(1)_Y$ , and 8 scalar candidate fields forming two isospin doublets of complex fields, ie 8 degrees of freedom. After spontaneous breaking of symmetry, there must remain three massive bosons:  $W^+$ ,  $W^-$  and  $Z$ , with 3 degrees of freedom each, a  $\gamma$  photon with 2 degrees of freedom and, by keeping the number of freedoms, 5 physical Higgs fields: 2 neutral CP-even:  $h$  and  $H$ , an CP-odd:  $A$ , and two Higgs charged  $H^\pm$ .

Table 5. Coupling of Higgs bosons to particles: leptons l, up (u,c,t) and down quarks (d,s,b), gauge bosons (V) for different Higgs doublet models (2HDM). The parameter  $\alpha$  is the mixing angle between neutral Higgs.

	$h\bar{U}U$	$h\bar{D}D$	$h\bar{E}E$	$H\bar{U}U$	$H\bar{D}D$	$H\bar{E}E$	$iA\bar{U}\gamma_5 U$	$iA\bar{D}\gamma_5 D$	$iA\bar{E}\gamma_5 E$
	$\kappa_h^u$	$\kappa_h^d$	$\kappa_h^e$	$\xi_H^u$	$\xi_H^d$	$\kappa_H^e$	$\kappa_A^u$	$\kappa_A^d$	$\kappa_A^e$
Type I	$\frac{\cos \alpha}{\sin \beta}$	$\frac{\cos \alpha}{\sin \beta}$	$\frac{\cos \alpha}{\sin \beta}$	$\frac{\sin \alpha}{\sin \beta}$	$\frac{\sin \alpha}{\sin \beta}$	$\frac{\sin \alpha}{\sin \beta}$	$-\cot \beta$	$\cot \beta$	$\cot \beta$
Type II	$\frac{\cos \alpha}{\sin \beta}$	$-\frac{\sin \alpha}{\cos \beta}$	$-\frac{\sin \alpha}{\cos \beta}$	$\frac{\sin \alpha}{\sin \beta}$	$\frac{\cos \alpha}{\cos \beta}$	$\frac{\cos \alpha}{\cos \beta}$	$-\cot \beta$	$-\tan \beta$	$-\tan \beta$
Type X	$\frac{\cos \alpha}{\sin \beta}$	$\frac{\cos \alpha}{\sin \beta}$	$-\frac{\sin \alpha}{\cos \beta}$	$\frac{\sin \alpha}{\sin \beta}$	$\frac{\sin \alpha}{\sin \beta}$	$\frac{\cos \alpha}{\cos \beta}$	$-\cot \beta$	$\cot \beta$	$-\tan \beta$
Type Y	$\frac{\cos \alpha}{\sin \beta}$	$-\frac{\sin \alpha}{\cos \beta}$	$\frac{\cos \alpha}{\sin \beta}$	$\frac{\sin \alpha}{\sin \beta}$	$\frac{\cos \alpha}{\cos \beta}$	$\frac{\sin \alpha}{\sin \beta}$	$-\cot \beta$	$-\tan \beta$	$\cot \beta$

At tree order, the Higgs sector is described by two parameters, chosen conventionally as the ratio  $\tan \beta = v_2/v_1$  of the expected values in the vacuum of the Higgs fields, as well as the mass of the CP-odd neutral Higgs boson,  $m_A$  for the search for neutral Higgs, or the mass of the charged Higgs for the search for charged Higgs. Thus, the Higgs couplings in the MSSM sector are increased for leptons  $\tau$  and b quarks, which motivates such channels for research. Some extensions of the Standard Model have been proposed for which the Higgs couplings differ from those of the Standard Model. For the MSSM, special case of the 2HDM model already mentioned, in addition to the description parameters in the order of the tree that constitute  $m_A$  and  $\tan \beta$ , other parameters come into play at the level of radiative corrections:  $m_{SUSY}$ ,  $M_2$ ,  $m_{\tilde{g}}$ ,  $\mu$ ,  $A_0$ :

- $m_{SUSY}$  is the mass parameter for soft supersymmetry breaking and represents a mass for scalar fermions (sfermions) on an electroweak scale;
- $M_2$  is the mass of gauginos on an electroweak scale
- $m_{\tilde{g}}$  is the mass of gluino;
- $\mu$  is the mass parameter of the Higgs
- $A_0 = A_t = A_b$  is the trilinear coupling

In addition, for scenarios with CP violation, the complex phases of  $A_0$  and  $m_{\tilde{g}}$ :  $\arg(A_0)$  and  $\arg(m_{\tilde{g}})$  are added. In addition to these parameters, the mass of the top quark, through radiative corrections, has a significant impact on predictions. The parameters for mixing the s-top and the s-bottom are defined respectively by:  $X_t = A_0 - \mu/\tan \beta$  and  $X_b = A_0 - \mu \tan \beta$ .

Under the hypothesis of the mass spectrum of Higgs particles of the MSSM compared to those of the Standard Model, different regimes can be considered, occupying different regions in the phase space in  $(m_A; \tan \beta)$ , leading to phenomenological consequences. According to the results in terms of LEP2 limit for the MSSM, the region not excluded corresponds to the decoupling regime. In this regime all the Higgs bosons, except the lightest ( $h$  in the MSSM), are heavier than the  $Z$  boson significantly, which corresponds to  $\cos(\beta - \alpha) \rightarrow 0$  and  $\sin(\beta - \alpha) \rightarrow 1$ . For the most general case of the 2HDM model with CP conservation, within the decoupling limit, the relative couplings compared to the Standard Model evolve as:

$$\frac{\cos \alpha}{\sin \beta} = \sin(\beta - \alpha) + \frac{\cos(\beta - \alpha)}{\tan \beta} \rightarrow 1 \tag{49}$$

that is to say a  $hUU$  coupling of the MSSM similar to that of the Standard Model;

$$\frac{\sin \alpha}{\sin \beta} = \cos(\beta - \alpha) - \frac{\sin(\beta - \alpha)}{\tan \beta} \rightarrow -\tan \beta^{-1} \tag{50}$$

that is to say an  $HUU$  coupling of the MSSM removed for the large  $\tan \beta$  values, which LEP2 promotes;

$$\sin(\beta - \alpha) \rightarrow 1 \tag{51}$$

that is to say an  $hVV$  coupling similar to that of the Standard Model.

$$\cos(\beta - \alpha) \rightarrow 0 \tag{52}$$

that is, a  $HVV$  coupling removed.

Taking into account the previous results and the zero coupling  $AVV$ , in the case of the decoupling regime favored by the results of LEP2, with large values of  $\tan \beta$ , for the neutral Higgs different from  $h$ , the couplings to quarks up (respectively at down quarks) are removed (increased respectively), while those with vector bosons are removed for  $H$  and  $h$ . Thus, the decays in pairs of  $b$ ,  $\tau$  and  $\mu$  are increased, the contribution of  $b$  quark is dominant in the virtual production loop  $gg \rightarrow H$ , the  $Hb\bar{b}$  coupling becomes dominant, in addition, the  $VBF$ ,  $WH$ ,  $ZH$  and  $Ht\bar{t}$  processes are suppressed. Thus, neutral Higgs bosons are produced mainly by two processes at the LHC: production in association with a  $b$  quark and by the fusion of gluons. The charged Higgs bosons are produced, for heavy Higgs ( $m_{H^\pm} > m_t$ ): mainly by the direct process  $gb \rightarrow tH^\pm$ , for Higgs of the order of  $m_{H^\pm} \equiv m_t$ : by fusion of gluons and by decaying of top quark:  $t \rightarrow bH^\pm$ , for light

Higgs ( $m_{H^\pm} < m_t$ ): by this same decaying of top quark.

For neutral Higgs bosons, excluding the channels with quark in the final state characterized by too much background noise, the channels considered are  $h/H/A \rightarrow \tau\tau$  and  $h/H/A \rightarrow \mu\mu$ , the second channel being characterized by a lower connection rate linked to the mass ratio  $\frac{m_\mu^2}{m_\tau^2}$  but a cleaner signature and a complete reconstruction of the mass of the Higgs. For heavy charged Higgs the dominant decay is  $H^\pm \rightarrow tb$  for large  $\tan\beta$  values,  $H^\pm \rightarrow \tau\nu$ . For light charged Higgs, the dominant decay is  $H^\pm \rightarrow \tau\nu$  for  $\tan\beta > 3$ . At small  $\tan\beta < 1$ , the channel  $H^\pm \rightarrow cs$  this is important with a branching ratio of around 40%.

The mass parameter  $\mu$  for supersymmetric Higgs (Higgsinos) appears in supersymmetric potential (superpotential) as a term of the form  $\mu H_u H_d$ . A naturalness problem appears, says  $\mu$  problem in this context, since the term  $\mu$ , the order of the electroweak scale, is by definition much weaker than the natural scale of break from theory, for example the Great Unification scale. An extension to the MSSM is the NMSSM which replaces the arbitrary  $\mu$  parameter with the expected value in a vacuum an additional scalar field, which removes the explicit scale in the Lagrangian.

The NMSSM also includes two pairs of complex scalar fields:

$$\Phi_1 = \begin{pmatrix} \phi_1 + i\phi_2 \\ \phi_3 + i\phi_4 \end{pmatrix}, \quad \Phi_2 = \begin{pmatrix} \phi_5 + i\phi_6 \\ \phi_7 + i\phi_8 \end{pmatrix}, \quad \phi_9 + i\phi_{10} \tag{53}$$

Before spontaneous symmetry breaking, there are 3 gauge fields  $W_{1,2,3}^\mu$  of massless  $SU(2)_L$  with two degrees of freedom each, a field of massless  $U(1)$ :  $B^\mu$  and 10 scalar candidate fields, i.e 10 degrees of freedom. After spontaneous breaking of symmetry, there must remain 3 massive bosons:  $W, Z$ , with 3 degrees of freedom each, a photon  $\gamma$  with 2 degrees of freedom and, by conservation of the number of freedom, 7 physical Higgs fields: 3 neutral peers in CP:  $h_1, h_2, h_3$ , two CP-odd neutral:  $a_1, a_2$ , two charged  $H^\pm$ . In the case of a search for the Higgs in the decay  $h_{1,2,3} \rightarrow aa \rightarrow 2\gamma + 2\gamma$ , the weak mass of the CP-odd neutral Higgs gives them a big push, collimating the photons of decay. Despite the significant granularity of a conventional detector in particle physics, it typically remains insufficient to separate the two photons from each Higgs boson has in separate clusters, which reconstructs such a signal as an effective decay  $h_{1,2,3} \rightarrow \gamma\gamma$ , artificially increasing this channel.

## 10. Conclusion

The large hadronic collider (LHC) recorded proton collisions corresponding to the energies of  $\sqrt{s} = 7\text{TeV}$  and  $\sqrt{s} = 8\text{TeV}$ . by the excellent collaboration of the two experiences ATLAS and CMS, a new resonance has been established, in particular at the channel  $h \rightarrow \gamma\gamma$ . Within the framework of the uncertainties and experimental delivered by LHC, the mass and the signal strength measured, the couplings, the quantum numbers, in particular the spin, the modes of production, the total and differential cross sections, are compatible with the Higgs boson of the Standard Model. The LHC was stopped in 2013 with the aim of restarting for run 2 at an energy of 13 TeV in 2015, in order to accumulate after 3 years about  $100\text{ fb}^{-1}$  of data. The measurement of the properties of the Higgs must continue, in particular by studying the possible deviations from the predictions of the Standard Model, but also by observing the channels for which individual discovery is not established:  $h \rightarrow \gamma\gamma$ ,  $h \rightarrow Z\gamma$  and  $h \rightarrow \mu\mu$ . Different perspectives are open to the channel  $h \rightarrow \gamma\gamma$ . The precise measurement of the Higgs mass is an important test of the Standard Model, to check its compatibility with indirect stresses, but also its consistency between the different decay channels. It helps to better understand the stable state of the vacuum, currently constrained as a metastable state. As part of the analysis of Higgs production measurements in the  $h \rightarrow \gamma\gamma$  channel of run 1 by LHC, the signal strength was measured with a relative accuracy of around 25%. The different couplings, in particular those corresponding to the rarest processes, are measured with much greater uncertainty. To explore the field of precision and to be able to discriminate between the Standard Model and new physics models, it is necessary to be able to reach relative details on the couplings of the order of about 5 - 10%. This is almost within reach of run 2, accumulating an integrated liminoity of about  $100\text{ fb}^{-1}$  at  $\sqrt{s} = 13\text{ TeV}$ .

## References

- [1] F. Englert and R. Brout. Broken symmetry and the mass of gauge vector mesons. *Phys. Rev. Lett.*, 13 :321-323 1964.
- [2] P. W. Higgs. Broken symmetries and the masses of gauge bosons. *Phys. Rev. Lett.*, 13 :508-509, Octobre 1964.
- [3] CMS Collaboration (S. Chatrchyan et al.). 2012 ecal detector performance plots. CMSDP-2013-007, Mars 2013.
- [4] S. L. Glashow. Partial symmetries of weak interactions. *Nucl. Phys.*, 22 :579-588, 1961.
- [5] A. Salam. Elementary particle theory : Relativistic groups and analyticity. Proc. of the 8th Nobel Symposium (Ed. N. Svartholm), Almqvist and Wiksell, Stockholm, pages 367-377, Mai 1968
- [6] S. Weinberg. A model of leptons. *Phys. Rev. Lett.*, 19 :1264-1266, Novembre 1967.
- [7] G. Arnison et al. Experimental observation of isolated large transverse energy electrons with associated missing energy at  $\sqrt{s} = 540$  GeV. *Phys. Lett. B*, 122 :103-116, Février 1983.
- [8] G. Arnison et al. Experimental observation of lepton pairs of invariant mass around 95 GeV at the cern sps collider. *Phys. Lett. B*, 126:398-410, Juillet 1983.
- [9] D. Karlen. The number of light neutrino types from collider experiments. *Phys. Lett. B*, 592 :445-446, Juillet 2004.
- [10] Y. Fukuda. Measurements of the solar neutrino flux from super-kamiokande's first 300 days. *Phys. Rev. Lett.*, 81 :1158-1162, Août 1998.
- [11] M. Apollonio et al. (CHOOZ Collaboration). Search for neutrino oscillations on a long baseline at the chooz nuclear power station. *Eur. Phys. J. C*, 27 :331-374, 2003.
- [12] N. Agafonova et al. (OPERA Collaboration). Observation of a first candidate in the opera experiment in the cngs beam. *Phys. Lett. B*, 691 :138-145, Juillet 2010.
- [13] K. Abe et al. (T2K Collaboration). First muon-neutrino disappearance study with an off-axis beam. *Phys. Rev. D*, 85 :031103(R), Février 2012.
- [14] J. et al. Particle Data Group Beringer. Review of particle physics (rpp). *Phys.Rev.D86* :010001
- [15] M. GellM. Gell-Mann. A schematic model of baryons and mesons. *Phys. Lett.*, 8 :214-215, 1964.-Mann. A schematic model of baryons and mesons. *Phys. Lett.*, 8 :214-215, 1964.
- [16] G. Zweig. An su(3) model for strong interaction symmetry and its breaking. Lichtenberg, D. B.(Ed.), Rosen, S. P. ( Ed.) : Developments In The Quark Theory Of Hadrons, Vol. 1, pages 22-101.
- [17] F. Abe et al. (CDF Collaboration). Observation of top quark production in antiprotonproton collisions with the collider detector at fermilab. *Phys. Rev. Lett.*, 74 :2626-2631
- [18] S. Abachi et al. (D0 Collaboration). Search for high mass top quark production in proton-antiproton collisions at  $\sqrt{s} = 1.8TeV$  . *Phys. Rev. Lett.*, 74 :2422-2426
- [19] O.V. ZO.V. Zenin V.V. Ezhela, S.B. Lugovsky. Hadronic part of the muon g-2 estimated on the sigma 2003(tot)( $e^+e^- \rightarrow hadrons$ ) evaluated data compilation.
- [20] S. Roth. *W* mass at lep and standard model fits.
- [21] The ALEPH Collaboration, the DELPHI Collaboration, the L3 Collaboration, the OPAL Collaboration, the SLD Collaboration, the LEP Electroweak Working Group, SLD electroweak, and heavy flavour groups. Precision electroweak measurements on the *Z* resonance.
- [22] Ch. Berger et al. PLUTO Collaboration. Evidence for gluon bremsstrahlung in  $e^+e^-$  annihilations at high energies. *Phys. Lett. B*, 86 :418-425
- [23] G. Senjanovic R. N. Mohapatra. Neutrino mass and spontaneous parity nonconservation. *Phys. Rev. Lett.*, 44 :912-915, 1980
- [24] Peter W. Higgs. Broken symmetries, massless particles and gauge fields. *Phys. Rev.Lett.*, 12 :132-133, Septembre 1964.



- [25] The LHC Higgs Cross Section Working Group (A. David et al.). Handbook of lhc higgs cross sections : 3. higgs properties.
- [26] A.D. Martin, W.J. Stirling, R.S. Thorne, and G. Watt. Parton distributions for the LHC. *Eur. Phys. J. C*, 63 :189-285.
- [27] Tilman Plehn. Lectures on LHC physics. *Lect. Notes Phys.*, 844 :1-193, 2012
- [28] Tilman Plehn. Lectures on LHC physics. *Lect. Notes Phys.*, 844 :1-193, 2012
- [29] M. Baak, M. Goebel, J. Haller, A. Hocker, D. Kennedy, R. Kogler, K. Monig, M. Schott, and J. Stelzer. The electroweak fit of the standard model after the discovery of a new boson at the LHC. *Eur. Phys. J. C*, 72 :2205-2217.
- [30] CMS Collaboration. Measurement of the properties of a higgs boson in the four-lepton final state.
- [31] CMS Collaboration. Updated measurements of the higgs boson at 125 gev in the two photon decay channel. CMS-PAS-HIG-13-001.
- [32] CMS Collaboration. Combination of standard model higgs boson searches and measurements of the properties of the new boson with a mass near 125 gev. CMS-PAS-HIG-13-005
- [33] The LHC Higgs Cross Section Working Group (A. David et al.). Lhc hxswg interim recommendations to explore the coupling structure of a higgs-like particle.
- [34] M. Quiros. Higgs bosons in extra dimensions.
- [35] M. Schmaltz. Physics beyond the standard model (theory) : Introducing the little higgs. *Nuc. Phys. B Proceedings Supplements*, 117 :40-49
- [36] H. E. Haber et D. O'Neil. Basis-independent methods for the two-higgs-doublet model.II. the significance of  $\tan \beta$ . *Phys. Rev. D*, 74 :015018
- [37] J. F. Gunion et H. E. Haber. Cp-conserving two-higgs-doublet model : The approach to the decoupling limit. *Phys. Rev. D*, 67 :075019
- [38] V. D. Barger, J. L. Hewett, and R. J. N. Phillips. New constraints on the charged higgs sector in two-higgs-doublet models. *Phys. Rev. D*, 41 :3421.
- [39] D. Graudenz et P.M. Zerwas M. Spira, A. Djouadi. Higgs boson production at the LHC. *Nucl. Phys. B*, 453 :17-82.
- [40] D.I. Kazakov. Supersymmetry on the run : LHC and dark matter. *Nucl. Phys. B Proceedings Supplements*, 203 :118-154.